Published in final edited form as:
J Phys Chem C Nanomater Interfaces. 2012 September 2; 116(5): 3845–3850. doi:10.1021/jp210582t.

Porphyrins-Functionalized Single-Walled Carbon Nanotubes Chemiresistive Sensor Arrays for VOCs

Mahendra D. Shirsat[†,#], **Tapan Sarkar**[†,#], **James Kakoullis Jr**[§], **Nosang V. Myung**[†], **Bharatan Konnanath**[‡], **Andreas Spanias**[‡], and **Ashok Mulchandani**[†,*]

[†]Department of Chemical and Environmental Engineering, University of California, Riverside, CA, USA.

[§]Department of Chemistry, University of California, Riverside, CA, USA.

[‡]School of Electrical, Computer and Energy Engineering, Arizona State University, Tempe, Arizona, USA

Abstract

Single-walled carbon nanotubes (SWNTs) have been used extensively for sensor fabrication due to its high surface to volume ratio, nanosized structure and interesting electronic property. Lack of selectivity is a major limitation for SWNTs-based sensors. However, surface modification of SWNTs with a suitable molecular recognition system can enhance the sensitivity. On the other hand, porphyrins have been widely investigated as functional materials for chemical sensor fabrication due to their several unique and interesting physico-chemical properties. Structural differences between free-base and metal substituted porphyrins make them suitable for improving selectivity of sensors. However, their poor conductivity is an impediment in fabrication of prophyrin-based chemiresistor sensors. The present attempt is to resolve these issues by combining freebase- and metallo-porphyrins with SWNTs to fabricate SWNTs-porphyrin hybrid chemiresistor sensor arrays for monitoring volatile organic carbons (VOCs) in air. Differences in sensing performance were noticed for porphyrin with different functional group and with different central metal atom. The mechanistic study for acetone sensing was done using field-effect transistor (FET) measurements and revealed that the sensing mechanism of ruthenium octaethyl porphyrin hybrid device was governed by electrostatic gating effect, whereas iron tetraphenyl porphyrin hybrid device was governed by electrostatic gating and Schottky barrier modulation in combination. Further, the recorded electronic responses for all hybrid sensors were analyzed using a pattern-recognition analysis tool. The pattern-recognition analysis confirmed a definite pattern in response for different hybrid material and could efficiently differentiate analytes from one another. This discriminating capability of the hybrid nanosensor devices open up the possibilities for further development of highly dense nanosensor array with suitable porphyrin for E-nose application.

Keywords

Single-Walled Carbon Nanotubes; Porphyrins; Chemiresistive; Nanosensor; Array; Volatile Organic Compounds

[*]Electronic mail of corresponding author: adani@engr.ucr.edu.
[#]these authors contributed equally

Supporting Information Available

Carrier concentration vs. resistance and mobility vs. resistance curves for bare and porphyrin coated SWNTs. This material is available free of charge via the internet at http://pubs.acs.org

Introduction

Single-walled carbon nanotube (SWNTs) has gained attention in sensing application owing to its unique electrical and structural properties.[1,2] In particular, the property of conductance change in SWNTs on absorption of analyte gas molecule makes it a potential material for sensor development.[3,4] Also, their high electrical mobility enables the development of low power microelectronics. Further, SWNTs, one-dimensional structure with a nanometer range diameter make it possible to develop a high-density nanosensor array within a limited space. However, lack of sensor performance in terms of sensitivity and selectivity is intrinsic in carbon chemistry and it limits the use of SWNTs as an individual sensor.[5] But surface modification of SWNTs with suitable guest molecule can enhance sensing performance. [6–8]

On the other hand, porphyrins are organic macrocyclic compounds having interesting structural and optical properties, and chemical stability.[9] They are able to bind nonspecifically with different analytes through Van der Waal forces, hydrogen bonding and coordination interaction with the central metal ion.[10,11] Further, changes in certain physical properties upon porphyrin-analyte binding makes porphyrins as an attractive class of sensing material. The sensing capabilities of porphyrin thin film have been demonstrated based on optical or mass detection.[12–16] Porphyrin thin-film based field-effect transistor (FET) also has been reported as a gas sensor.[15,17] Although, the transduction mechanisms of the above mentioned device are simple, fabrication may require use of complex technology. In this regard, chemiresistive sensor based on conductivity change could be the simplest possible transduction mechanism, which requires simple technology for electronic application. Very low electrical conductivity of the porphyrin structure makes it difficult to develop only porphyrin based chemiresistive sensor.[18] However, SWNTs-porphyrin hybrid, which can be prepared by surface modification of SWNTs with porphyrin, could overcome the conductivity issue. In SWNTs-porphyrin hybrid, the high electrical mobility of SWNTs improves the device conductance, whereas, the binding ability of porphyrin towards different analyte improves sensing performance of the hybrid device when used as a sensory layer.

Porphyrin has a flat and planar structure that facilitates π-π interaction and bind to the SWNTs surface almost without altering SWNTs electronic properties.[19] Further, porphyrin can be easily tailor-made at the synthetic level by adding different functional groups at the outer porphyrin ring and by introducing different metal atoms at the core of the porphyrin ring which could provide different transduction mechanism depending upon the type of interaction between the porphyrin and analyte. The richness of porphyrin library facilitates to develop independently SWNTs-porphyrin hybrid based sensors array. There are reports on multi-walled carbon nanotubes (MWCNTs) based porphyrin hybrid sensor for sensing volatile organic compound (VOCs).[20] However, it requires complex sensor fabrication techniques. Also it lacks to explain the possible sensing mechanism.

In this work, we report a nanosensor array based on porphyrins-functionalized SWNTs hybrids operating in chemiresistive mode for a wide spectrum of VOCs. Various porphyrins viz. octaethyl porphyrin (OEP), ruthenium OEP (RuOEP), iron OEP (FeOEP), manganese OEP (MnOEP), tetraphenyl porphyrin (TPP), ruthenium TPP (RuTPP) and iron TPP (FeTPP) were used for surface modification of SWNTs. Systematic study was done to evaluate sensing performance of the hybrid devices towards a number of VOCs. Field-effect transistor (FET) analysis was done to understand the sensing mechanism of the hybrid device. Principle component analysis (PCA) was done using sensing data of hybrid devices to determine the discrimination capability of the devices towards different VOCs. PCA results revealed clear segregation of sensing response to each gas thus providing a unique signature of responses of different devices towards various VOCs.

Methods

Nanosensor Fabrication

SWNT solution was prepared dispersing 0.2 mg of carboxylated SWNTs [P3 SWNT-COOH 80 ~ 90% purity from Carbon Solution Inc. (Riverside, CA, USA)] in 10 ml of N,N-dimethylformamide (DMF) (Sigma Aldrich, Spectral grade) by ultrasonication for 90 minutes followed by centrifugation at 31,000 g for another 90 minutes to separate soluble fraction from the aggregates.

Sensor arrays were microfabricated on highly doped p-type silicon substrate by standard lithographic patterning. First, approximately 100 nm SiO_2 insulated layer was deposited on the substrate by low-pressure chemical vapor deposition (LPCVD). Electrodes were written on the substrate by photolithography, followed by the deposition of 20 nm Cr layer and 180 nm of Au layer by e-beam evaporation. The width of the electrode was 200 nm and separated by a gap of 3 μm. Finally electrodes were defined by using standard lift-off technique.

To bridge the gap between the gold electrodes, SWNTs were aligned dielectrophoretically across the electrodes by putting 0.1 μl of SWNT suspended solution on the top of the electrode gap while applying 3 V_{P-P} at 4 MHz frequency by a function generator (Wavetek, San Diego, CA, USA). Desirable resistance of the device could be achieved by varying the alignment time. After alignment, the device was washed with nanopure water to remove the extra SWNTs solution and dried by gently blowing dry nitrogen gas. The electrode was then annealed at 300°C for 90 minutes under reducing environment (5% H_2 in N_2) to improve the contact between the gold electrode and SWNTs by removing any DMF residues between electrode and SWNTs.

SWNTs were functionalized with different free-base and metal substituted porphyrin by solvent casting technique. A 0.1 mM porphyrin solution was prepared in DMF for each porphyrin.

Gas Sensing Studies

For gas sensing studies, the sensors were wire-bonded (West Bond Inc., Anaheim, CA, USA) to a chip holder, and each sensor was connected in series with a potentiometer. The value of the potentiometer was adjusted to a near possible value of the initial resistance of the sensor to optimize the resolution obtained from the measurement. A bias potential of 1 V was applied across the sensor to study the sensing performance. The sensor was covered with a 1.3 cm^3 sealed glass dome of with gas inlet and outlet. Dry air (purity: 99.998%, Air gas Inc., Riverside, CA, USA) was used as carrier gas. Saturated VOCs vapor was generated by passing dry air though a bubbler filled with liquid VOCs. Different concentration of VOCs vapor was obtained by mixing VOCs vapor stream and dry air. Two mass flow controllers (Alicate Scientific Inc, Tucson, AZ, USA) were used to control the gas flow rate. A Labview program was developed in-house and used to control and monitor the voltage of the circuit using a field point analog input and outputs modules (National Instruments, Austin, TX, USA). In all the experiments, sensors were first exposed to dry air to achieve the baseline, then to a desired concentration of analyte vapor concentration, and then back to air, which completed one cycle.

Characterization

The structural characterization of SWNTs-porphyrin hybrid device was done by using scanning electron microscope (XL-30 FEG, FEI, Oregon, USA) and atomic force microscope (Veeco Innova, Santa Barbara, CA, USA).

Electrical characterization was done through current-voltage (I_{DS}-V_{DS}) measurement and field-effect transistor (FET) measurement, to confirm surface functionalization of SWNTs with RuOEP. FET measurements were also performed for elucidation of the sensing mechanism by exposing the device to air or saturated vapors of acetone and DCM. The I_{DS}-V_{DS} for device was measured by linear sweep voltammetry using electrochemical analyzer (CHI model 1202A, Austin, TX, USA) and FET measurement was done by using a semiconductor parameter analyzer (HP model # 4155A, Palo Alto, CA, USA). For FET measurements, the gold electrodes served as drain and source while the aligned SWNTs/aligned modified SWNTs acted as channel. Back gate potential was applied through the highly doped Si surface. A 100 nm thick dielectric layer of SiO_2 used to separate the back gate from source-drain. The source-drain current (I_{DS}) was measured at room temperature as a function of applied gate voltage (V_G).

Results

Verification of Porphyrin-SWNTs Hybrid Formation

The formation of porphyrins-SWNT hybrid was verified by microscopy (SEM and AFM) and electrical (I_{DS}-V_{DS} and I_{DS}-V_G, FET) studies of Ru-OEP functionalized device. The Ru peak in the energy dispersive X-ray (EDAX) spectrum [Fig. 1a] of the corresponding SEM image [Fig. 1a, inset] confirmed the presence of Ru in Ru-OEP coated SWNTs. Similarly, the AFM analyses revealed an increase in the average diameter of the bare SWNTs from ~3.5 nm to ~7.5 nm after functionalization with RuOEP [Fig. 1b].

The modulation of resistance/conductance, threshold gate voltage and transconductance of the SWNTs is a facile method for verifying functionalization of SWNTs. Figure 2 shows the I_{DS}-V_{DS} and I_{DS}-V_G (FET) characteristics of bare and Ru-OEP functionalized SWNTs. As shown in the Fig. 2a, the conductance of bare SWNTs device decreased significantly upon functionalization with RuOEP. Further, the RuOEP-coated SWNTs device had a more negative threshold gate voltage (V_{TH}) and lower transconductance when compared to the bare SWNTs device. These changes are attributed to the n-doping by the electron donor porphyrin[21–23] of the p-type semiconductor SWNTs[2,3] that results in lower carrier (hole) concentration[21–23] [Fig. S1(a)] and carrier mobility [Fig. S1(b)].

VOCs Sensing

In order to evaluate the potential of porphyrins-functionalized SWNTs arrays for discriminating VOCs, room temperature responses (defined as $\Delta R/R_o$ % = $(R-R_o)/R_o$ *100; where R= resistance of the device exposed to analyte and R_o is the initial base line resistance before analyte exposure) of various SWNTs-porphyrins hybrid sensors as a function of concentration to a wide range of VOCs such as acetone, ethanol (EtOH), methanol (MeOH), methyl ethyl ketone (MEK), and dichloromethane (DCM), and water vapor were investigated.

Figure 3 illustrates a sample calibration plot along with the dynamic response (inset) of the SWNTs-OEP hybrid for MEK detection. The data shows a fast responding sensor with the response attaining 60% and 90% of the maximum in less than 1 min. and 7.2±1.9 min., respectively (Fig. 3, inset). Similar fast responses were observed for other porphyrin-functionalized SWNTs devices with MEK and other VOCs tested (data not shown). Further, OEP-functionalized SWNTs device was significantly more sensitive compared to the bare SWNTs device. However, the improved sensitivity was not limited to SWNTs-OEP and not all the porphyrins coatings improved SWNTs sensitivity to MEK. As shown in Fig. 4, RuOEP-, FeOEP- and MnOEP-SWNTs hybrid sensors were less sensitive, whereas, OEP-, TPP-, RuTPP- and FeTPP-SWNTs hybrid devices were more sensitive than bare SWNTs

sensor for MEK. A similar non-selective response pattern was observed from porphyrins-functionalized SWNTs hybrid sensors in the array for other VOCs tested in this work [Fig. 4]. Thus, each analyte has a somewhat distinct response pattern/signature making its identification/detection feasible by combining with chemometric analysis. The pattern/signature of each vapor can be attributed to the diversity of the sensing elements, i.e. porphyrins, with different peripheral ligand and central metal. The exact role of the different functional groups of porphyrins in generating the signature is not well understood and would require a more systematic investigation for elucidation. It is also worth noting that both Ru-OEP and Ru-TPP functionalized SWNT devices did not respond to water vapor, which should be helpful for the success of sensor array in ambient environment where water vapor is present.

Sensing Mechanism

The above sensing responses of porphyrin-SWNTs hybrid devices can be ascribed to one or more of the following: electrostatic gating due to charge transfer, Schottky barrier modification resulting from work function change and reduced charge mobility by the introduced scattering sites.[24] Reports in literature on porphyrin-functionalized CNTs devices for gas sensing proposed a charge transfer mechanism for the sensor response without any evidence.[11,20] In order to shed light on the sensor mechanism, FET measurements were carried out for SWNTs-RuOEP and SWNTs-FeTPP upon exposure to dry air or saturated vapors of acetone. As evident from Fig. 5a, there was a positive shift of ~5V of threshold gate voltage (V_{TH}) with respect of air when SWNTs-RuOEP hybrid was exposed to acetone. Acetone is an electron donating species and thus exposure to acetone causes a shift in valence band away from the Fermi level resulting in a decrease in charge carrier (hole) concentration[25] (~3.3×10^{10} cm^{-1}), thereby reduction in conductivity and negative shift in threshold voltage (V_{TH}) of the device. In comparison, the mobility (calculated from the device transconductance, slope of the I_{DS} vs. V_G) of the SWNTs-RuOEP device in air, and saturated acetone were ~3.6×10^{-2} and ~4.1×10^{-2} $cm^2V^{-1}s^{-1}$, respectively.[26] Thus, the change in V_{TH} as well as carrier concentration is significant in magnitude when compared to mobility for acetone indicating that the sensing mechanism for SWNTs-RuOEP hybrid is governed by electrostatic gating effect.[27]

Figure 5b shows the FET transfer characteristics for the FeTPP-functionalized SWNT device. Once again, like SWNTs-RuOEP, a negative shift in of 11.4 V in the gate voltage with respect to air was observed upon exposure to saturated vapors of acetone. This corresponds to a carrier concentration change of ~2.8×10^{10} cm^{-1} in acetone environment compared to air. However, unlike SWNTs-RuOEP device, there was a significant change in the mobility of the SWNTs-FeTPP upon exposure to acetone (~4.9 $cm^2V^{-1}s^{-1}$) compared to air (1.1 $cm^2V^{-1}s^{-1}$). This 4-fold change in mobility indicates a decrease in work function of the device on absorption of analyte gas at the gold contact causing Schottky barrier modulation.[27] Thus, a threshold voltage shift and mobility change in case of SWNTs-FeTPP hybrid device suggests that the sensing mechanism is governed by electrostatic gating and Schottky barrier effect in combination.[27]

Principal Component Analysis

To evaluate the VOCs identification performance of porphyrins-SWNT hybrid sensors array, the simple statistical chemometric technique of principal component analysis (PCA) was used. A data matrix was constructed whose columns were the peak responses from 7 sensors (SWNTs, SWNTs-OEP, SWNTs- RuOEP, SWNTs-FeOEP, SWNTs-TPP, SWNTs-RuTPP, and SWNTs-FeTPP) and the rows represented measurements for each gas. For each gas, 3 measurements (corresponding to 100%, 75% and 50% saturated vapors) were selected. Thus, the data matrix had 15-rows and 7-columns. Multivariate analysis was

carried out performing principal component analysis (PCA). PCA is an orthogonal projection of data from a higher dimensional space to a lower dimensional one such that the variance of the projected data is maximized. In our case, we found that first 3 principal components (PCs) accounted for ~88% of the variance. Visual analysis was enabled by plotting the scores the projection of the data points in the PC space. The first principal component (PC1) contained information about the concentration of the analyte. As shown in Fig. 6(a), concentration of each analyte increased as the magnitude of PC1 increased and followed a definite trend between different concentrations of analytes. Further, PCA plot of the second (PC2) and third principal components (PC3) provided information about the discriminatory power of the sensors. It can be observed from Fig. 6(b) that the scores representing each gas were clustered together and there was a clear separation between the clusters corresponding to each gas.

Conclusions

To summarize, we have fabricated single-walled carbon nanotubes-porphyrins hybrid based chemiresistive nanosensor array for monitoring toxics in the environment. Differences in sensing performance are observed for porphyrin with different functional group and with different central metal atom. Freebase and metal (e.g. ruthenium and iron) substitution with octaethyl and tetraphenyl porphyrins provide good selectivity and sensitivity to various VOCs under test. The FET analysis revealed that the sensing mechanism of SWNTs-RuOEP device is governed by electrostatic gating effect and for SWNTs-FeTPP, it is electrostatic gating and Schottky barrier modulation in combination. However, Schottky barrier modulation is dominant over electrostatic gating effect in case of SWNTs-FeTPP device. Further, the test data generated by the hybrid nanosensor array was analyzed using PCA technique. PCA analyses confirmed the presence of definite pattern in response data for different hybrid material and ability to differentiate analyte from others. This discriminating power of the hybrid devices and availability of the wide range of commercially available synthetic porphyrin, open up an opportunity to develop a highly dense nanosensor array for E-nose application.

Supplementary Material

Refer to Web version on PubMed Central for supplementary material.

Acknowledgments

This material is based on research sponsored by the National Institutes of Health Genes, Environment and Health Initiative through the award U01ES016026. The United States government is authorized to reproduce and distribute reprints for government purposes, not withstanding any copyright notation thereon. MS expresses his gratitude to the Dr. Babasaheb Ambedkar Marathwada University, Aurangabad, India for the sanction of study leave. TS is grateful to Govt. of INDIA for his financial assistance.

References

1. Baughman RH, Zakhidov AA, de Heer WA. Science. 2002; 297:787. [PubMed: 12161643]
2. Kong J, Franklin NR, Zhou C, Chapline MG, Peng S, Cho K, Dai H. Science. 2000; 287:622. [PubMed: 10649989]
3. Collins PG, Bradley K, Ishigami M, Zettl A. Science. 2000; 287:1801. [PubMed: 10710305]
4. Snow ES, Perkins FK, Houser EJ, Badescu SC, Reinecke TL. Science. 2005; 307:1942. [PubMed: 15790850]
5. Zhang T, Mubeen S, Myung NV, Deshusses MA. Nanotechnology. 2008; 19:332001. [PubMed: 21730614]
6. Kong J, Chapline MG, Dai H. Adv. Mater. 2001; 13:1384.

7. Zhang T, Nix MB, Yoo BY, Deshusses MA, Myung NV. Electroanalysis. 2006; 18:1153.
8. Zhang T, Mubeen S, Bekyarova E, Yoo BY, Haddon RC, Myung NV, Deshusses MA. Nanotechnology. 2007; 18:165504.
9. Biesaga M, Pyrzynska K, Trojanowicz M. Talanta. 2000; 51:209. [PubMed: 18967853]
10. Di Natale C, Monti D, Paolesse R. Materials Today. 2010; 13:46.
11. Penza M, Rossi R, Alvisi M, Signore MA, Serra E, Paolesse R, D'Amico A, Di Natale C. Sens. Actuators B. 2010; 144:387.
12. Akrajas, Mat Salleh M, Yahaya M. Sens. Actuators B. 2002; 85:191.
13. Rakow NA, Suslick KS. Nature. 2000; 406:710. [PubMed: 10963592]
14. Lim SH, Feng L, Kemling JW, Musto CJ, Suslick KS. Nature Chem. 2009; 1:562. [PubMed: 20160982]
15. Di Natale C, Buchholt K, Martinelli E, Paolesse R, Pomarico G, D'Amico A, Lundstrom I, Lloyd Spetz A. Sens. Actuators B. 2009; 135:560.
16. Kim J, Lim S-H, Yoon Y, Thangadurai TD, Yoon S. Tetrahedron Lett. 2011; 52:2645.
17. Andersson M, Holmberg M, Lundstrom I, Lloyd-Spetz A, Martensson P, Paolesse R, Falconi C, Proietti E, Di Natale C, D'Amico A. Sens. Actuators B. 2001; 77:567.
18. Tanaka H, Yajima T, Matsumoto T, Otsuka Y, Ogawa T. Adv. Mater. 2006; 18:1411.
19. Rahman GMA, Guldi DM, Campidelli S, Prato M. J. Mater. Chem. 2006; 16:62.
20. Penza M, Alvisi M, Rossi R, Serra E, Paolesse R, D'Amico A, Natale CD. Nanotechnology. 2011; 22:125502. [PubMed: 21325715]
21. Itkis ME, Niyogi S, Meng ME, Hamon MA, Hu H, Haddon RC. Nano Lett. 2002; 2:155.
22. Strano MS, Huffman CB, Moore VC, O'Connell MJ, Haroz EH, Hubbard J, Miller M, Rialon K, Kittrell C, Ramesh S, Hauge RH, Smalley RE. The J. Phys. Chem. B. 2003; 107:6979.
23. Kauffman DR, Kuzmych O, Star A. The J. Phys. Chem. C. 2007; 111:3539.
24. Kauffman DR, Star A. Angew. Chem. Int. Ed. 2008; 47:6550.
25. Snow ES, Campbell PM, Ancona MG, Novak JP. Appl. Phys. Lett. 2005; 86:033105.
26. Lim J-H, Phiboolsirichit N, Mubeen S, Deshusses MA, Mulchandani A, Myung NV. Nanotechnology. 2010; 21:075502.
27. Heller I, Janssens AM, Mannik J, Minot ED, Lemay SG, Dekker C. Nano Lett. 2008; 8:591. [PubMed: 18162002]

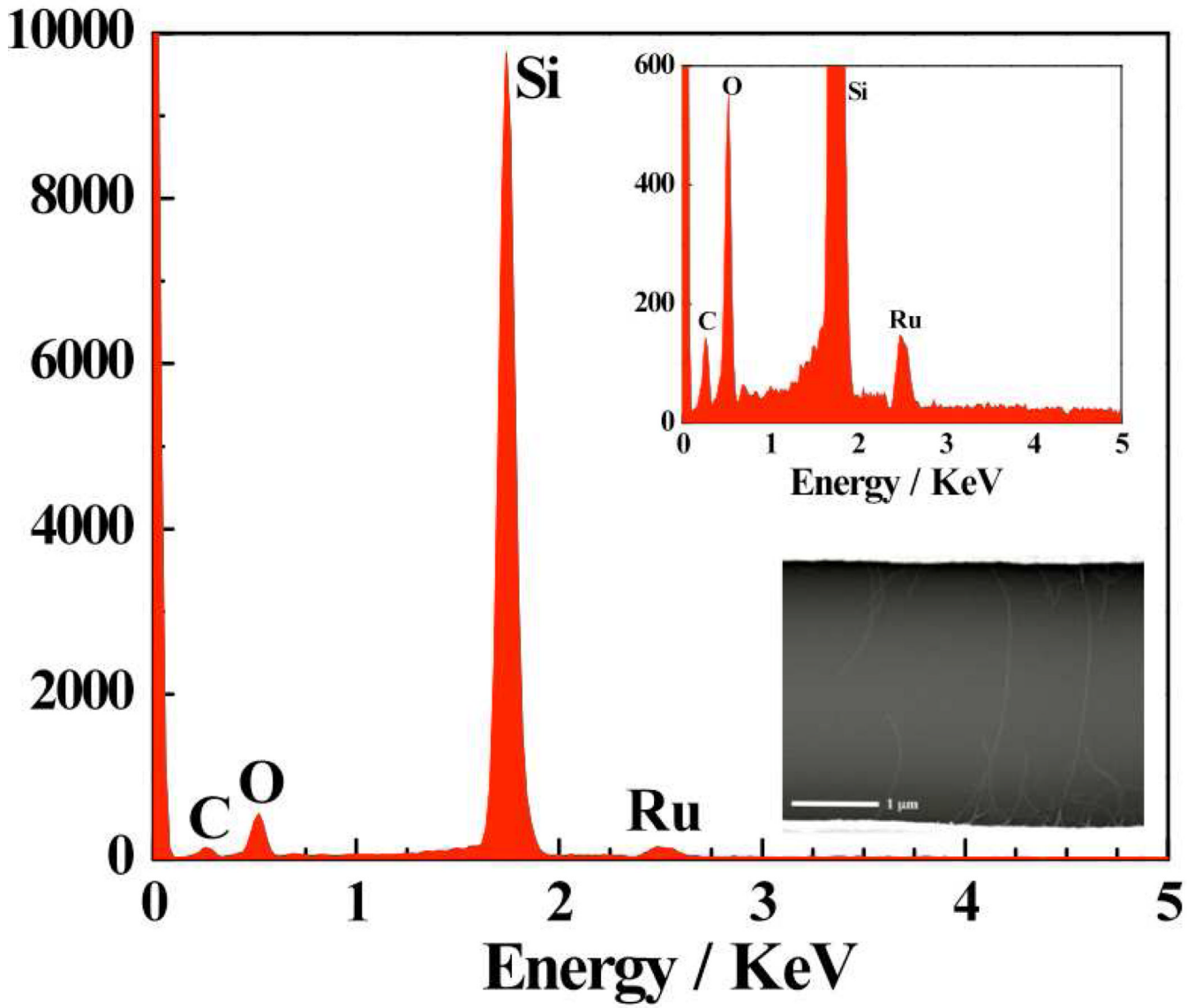

1(a)

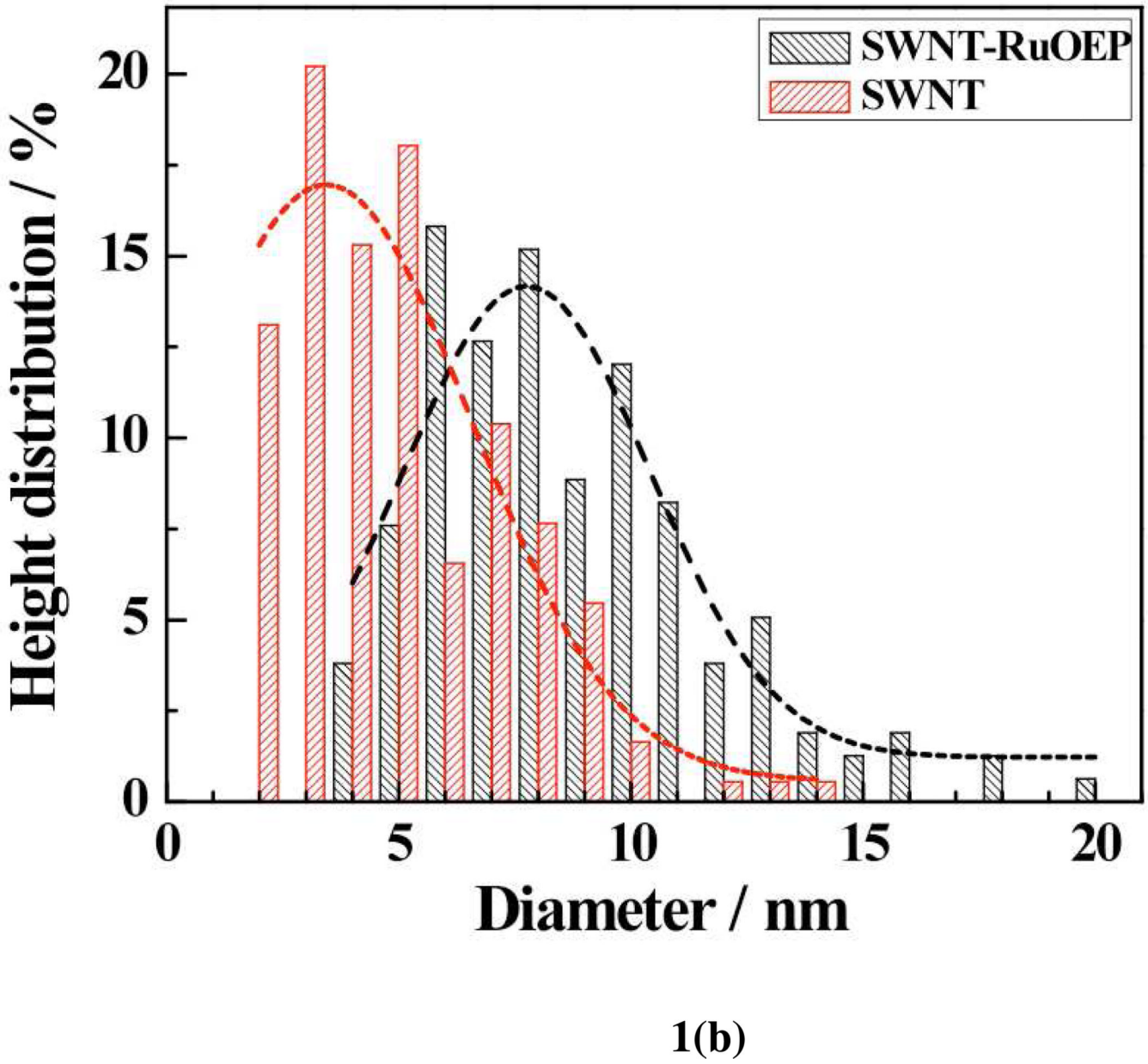

1(b)

Figure 1.
(a) Energy dispersive X-ray analysis (EDAX) spectrum and SEM image of RuOEP coated SWNT (inset); (b) Height distribution of bare and SWNTs-RuOEP device obtained from AFM analysis.

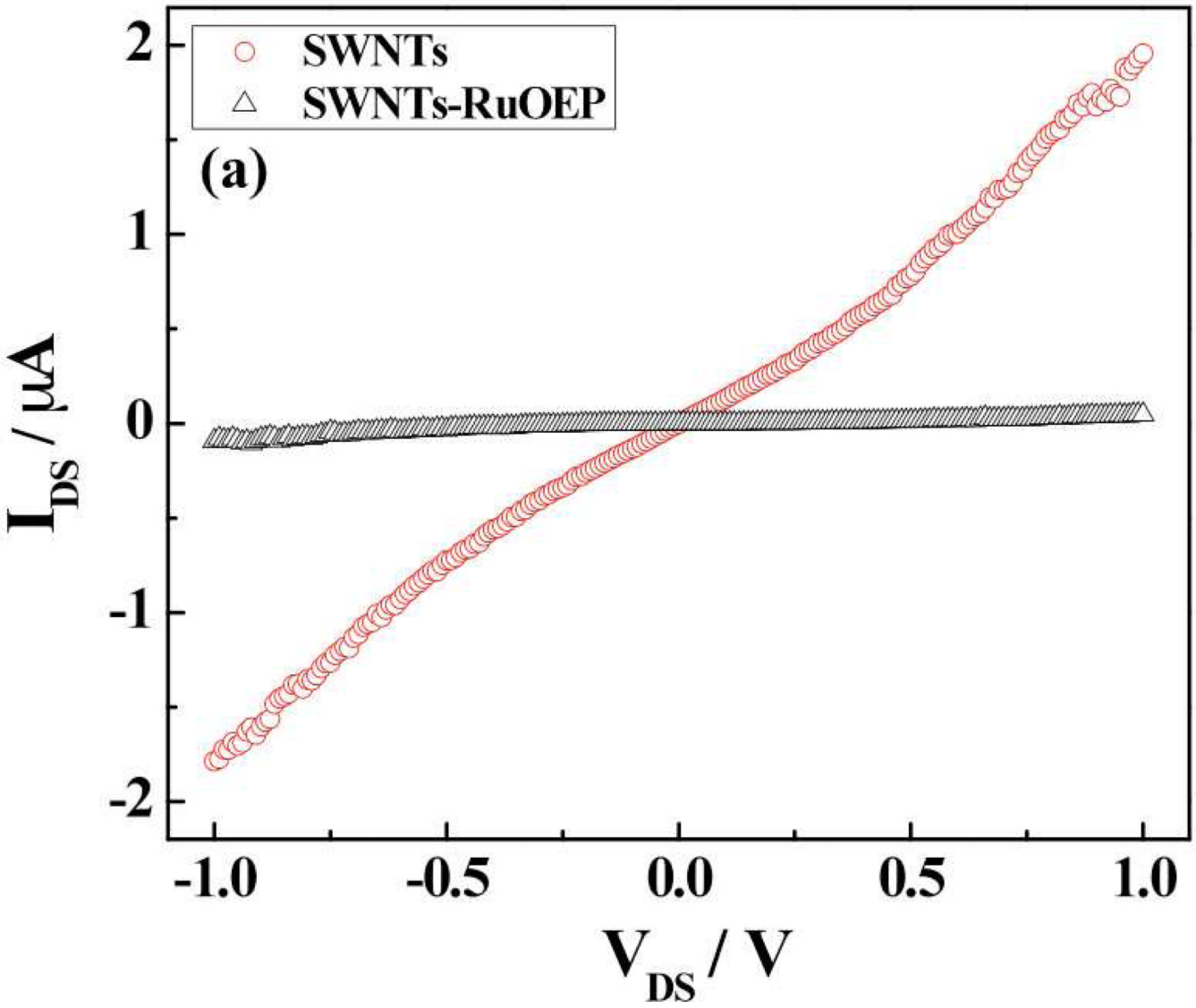

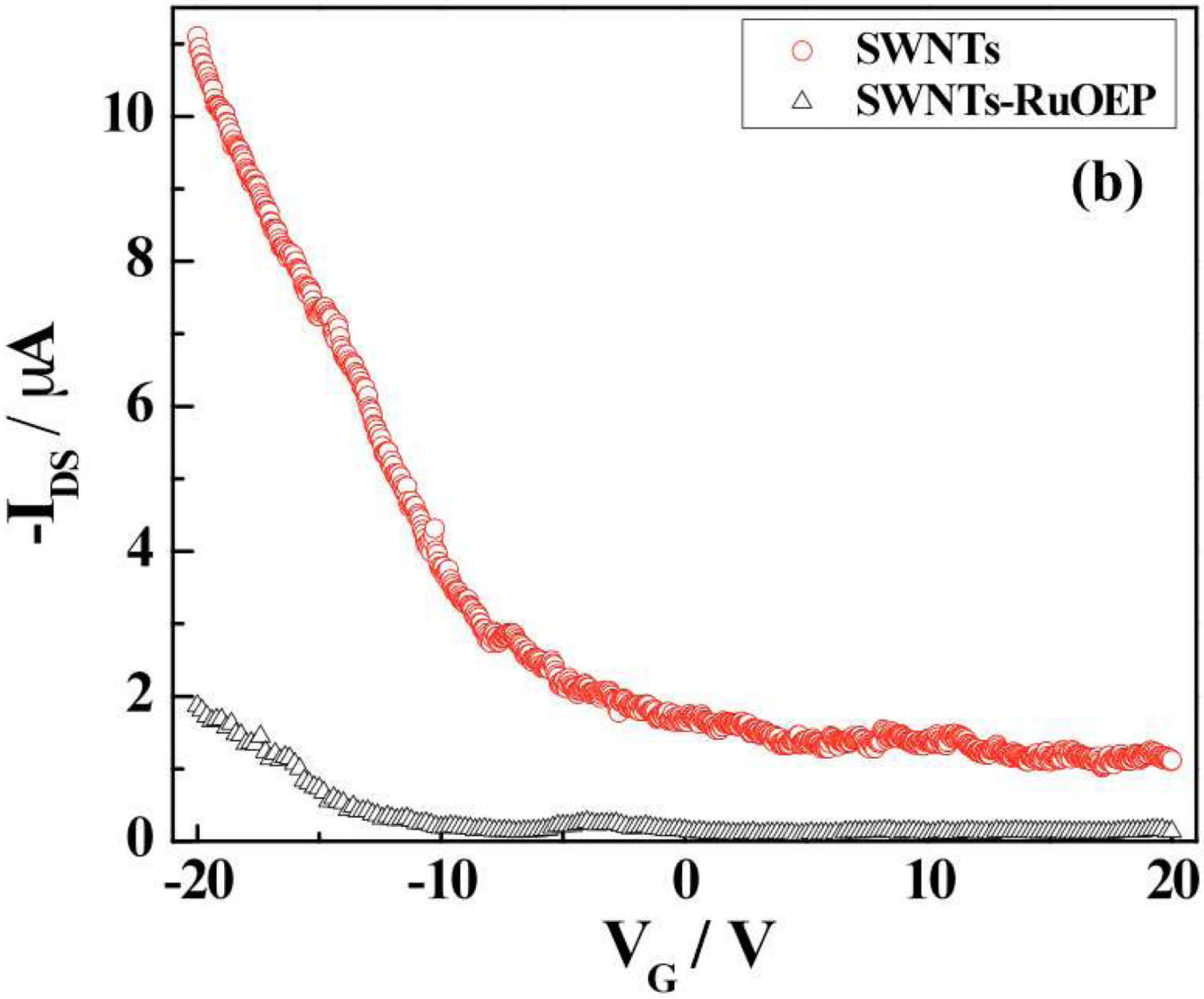

Figure 2.
Electrical and FET transfer characteristics of bare and RuOEP-functionalized SWNTs device: a) I_{DS}- V_{DS} curve (at V_{GS} = 0 V) and b) I_{DS} – V_{GS} curve (at V_{DS}= −1 V).

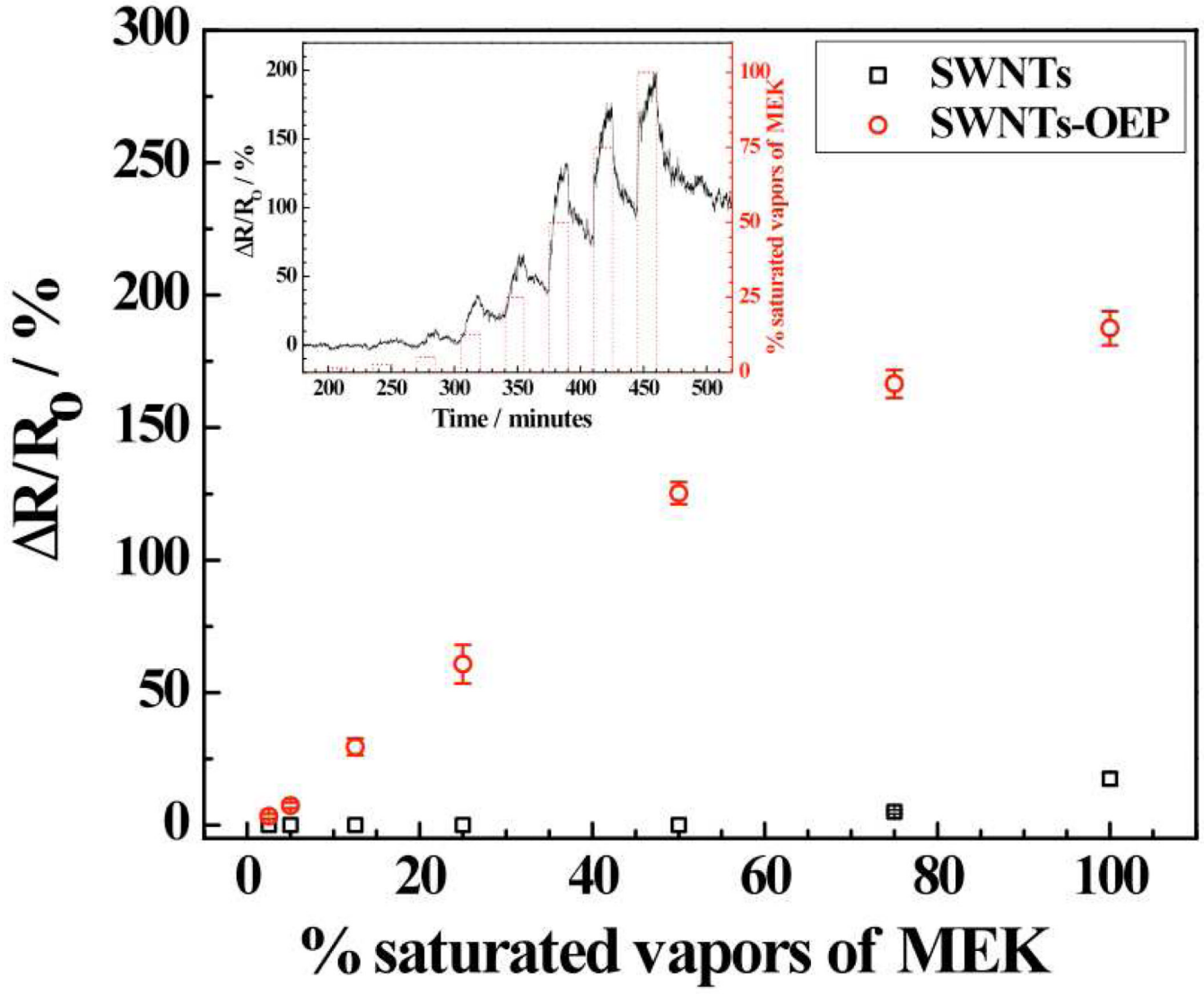

Figure 3.
Calibration curves of MEK for bare SWNT and freebase and metal substituted porphyrin functionalized devices and transient response of MEK for SWNTs-RuOEP device (inset).

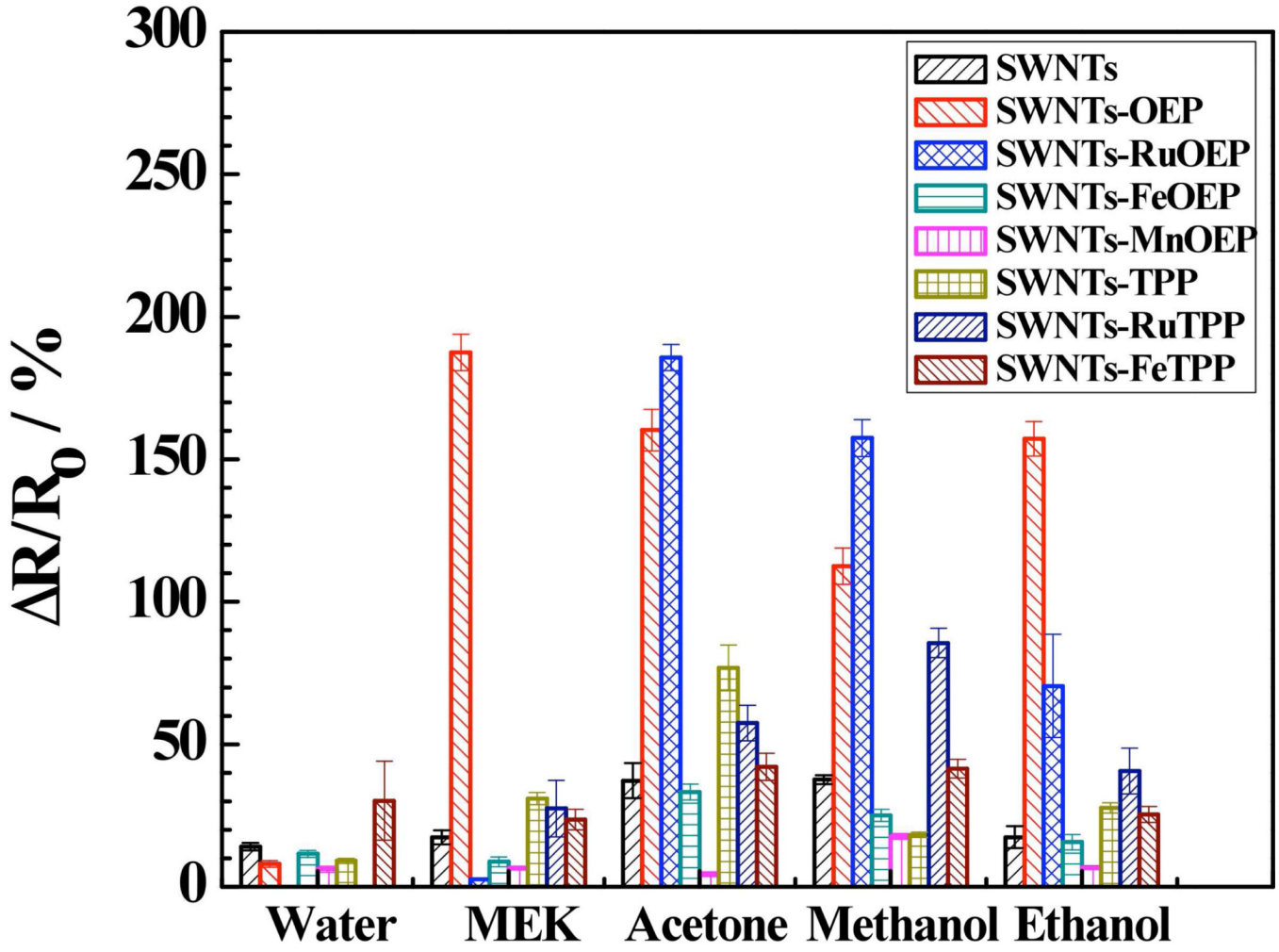

Figure 4.
Histogram showing comparison of responses of bare and freebase and metal substituted functionalized devices towards acetone, methanol, ethanol, MEK and water (@100% saturated vapors).

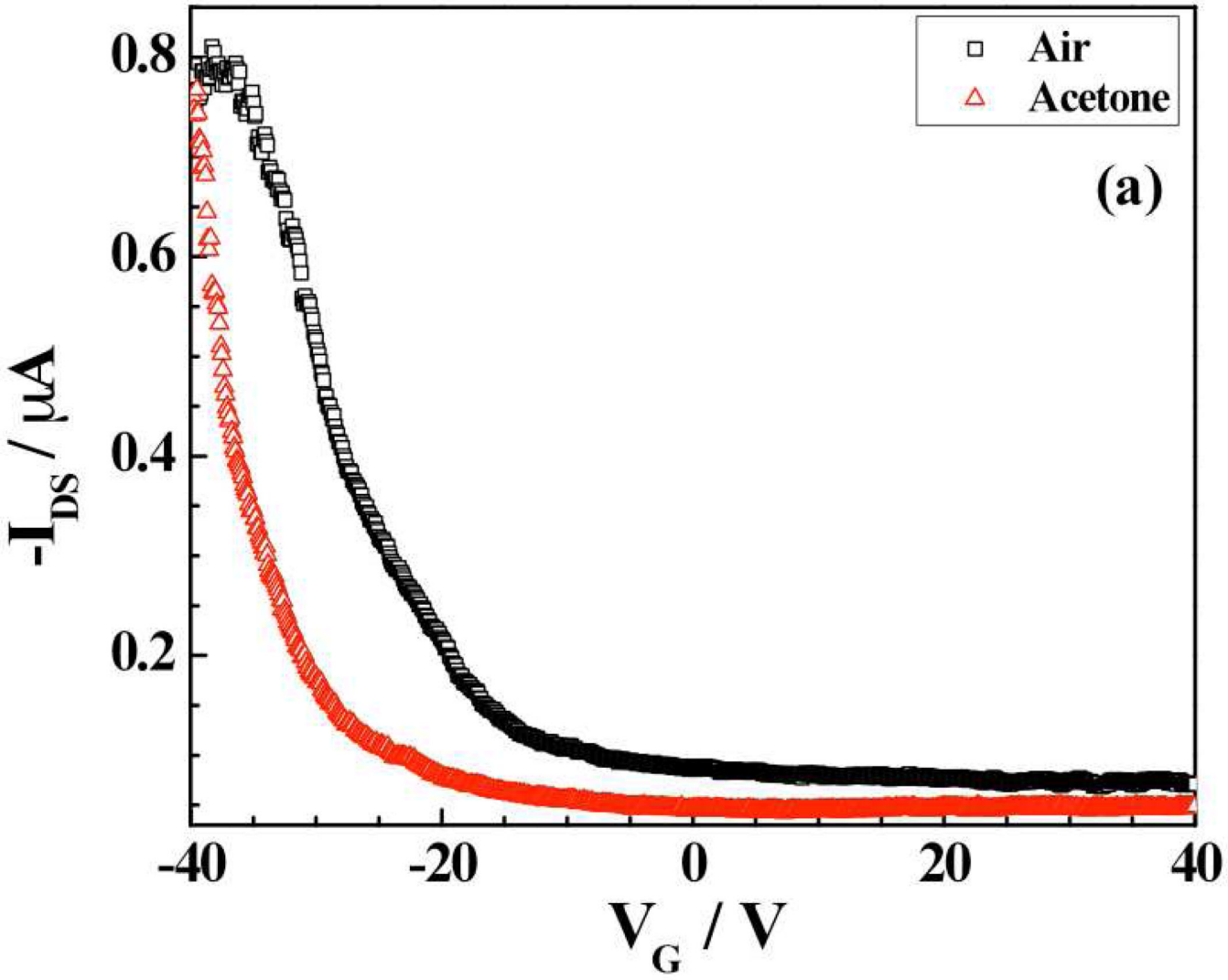

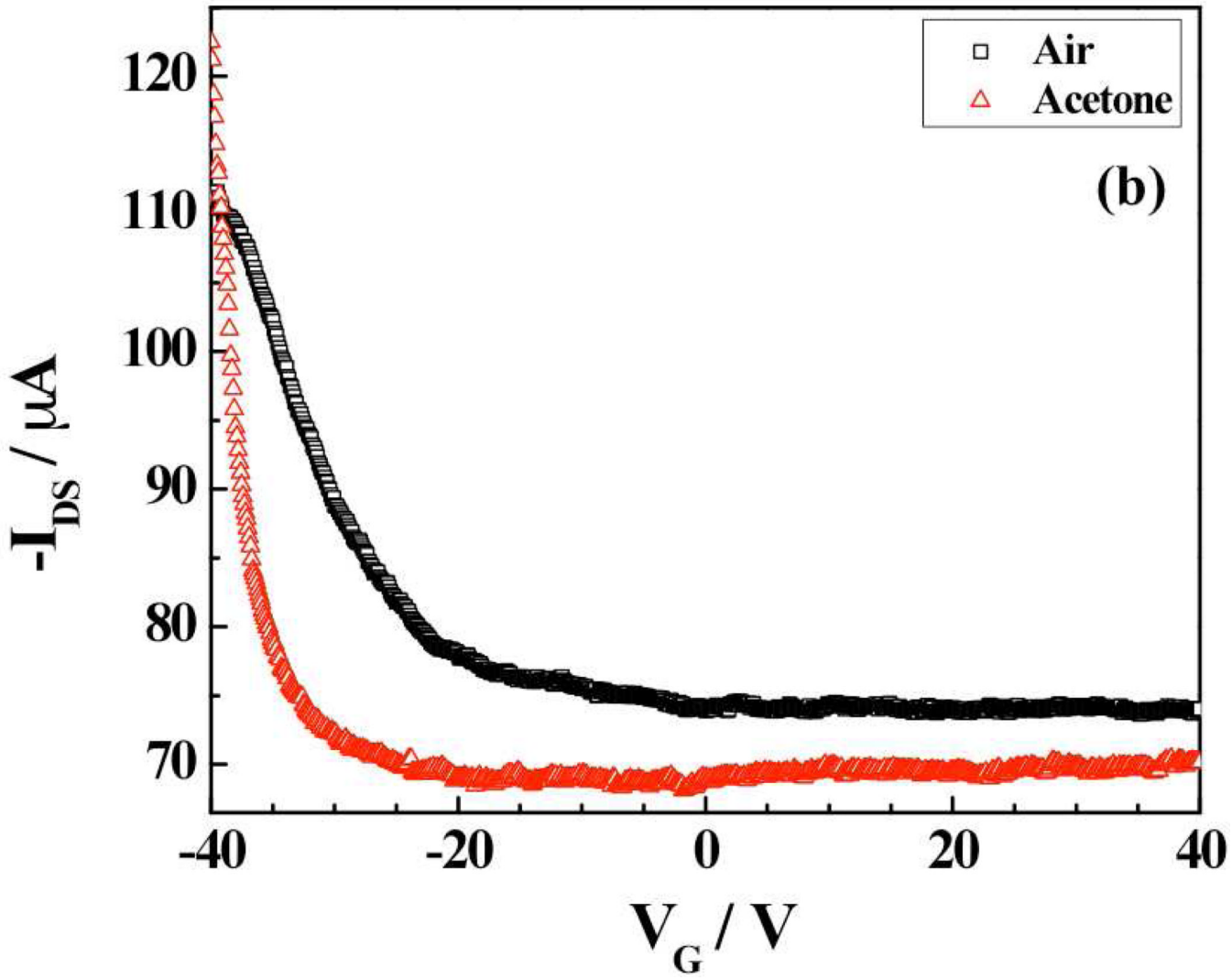

Figure 5.
Transfer characteristic (I_{DS} - V_{GS} curves at V_{DS} = − 1 V) of (a) SWNTs-RuOEP and (b) SWNTs-FeTPP device in presence of air and saturated vapors of acetone.

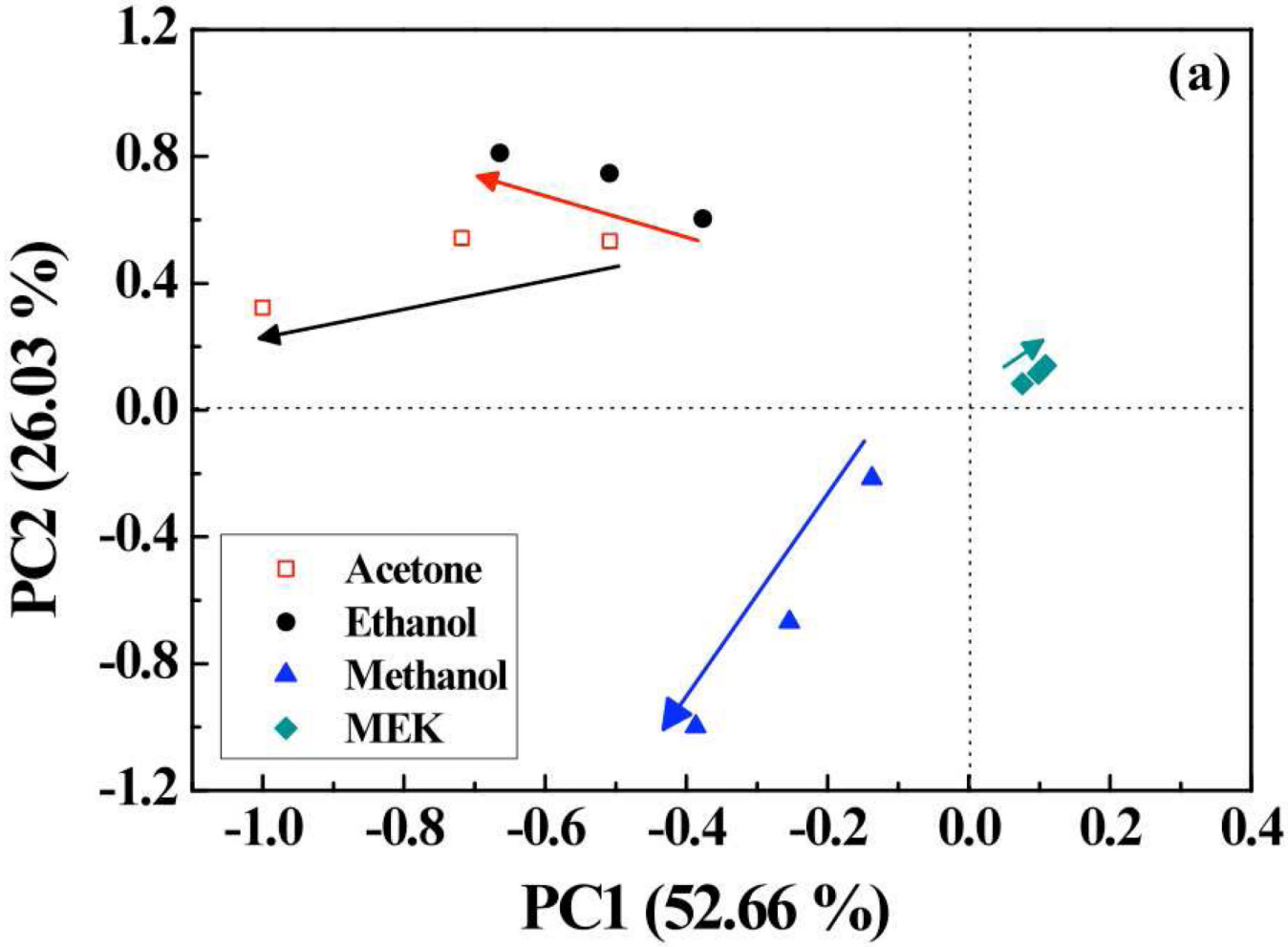

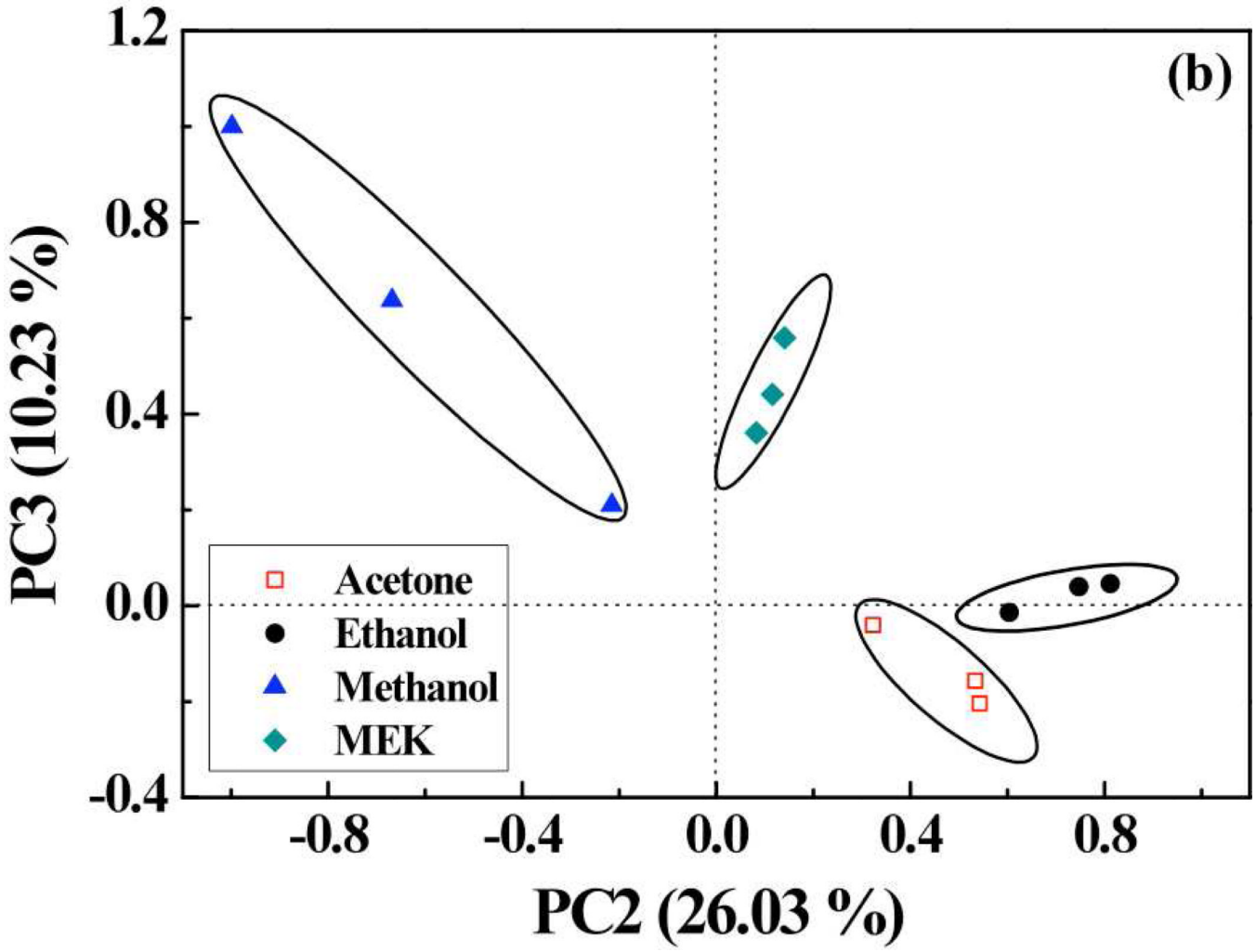

Figure 6.
(a) PCA plot (PC1 vs. PC2) of scores using 7 sensors (bare SWNT, SWNTs-OEP, SWNTs-RuOEP, SWNTs-FeOEP, SWNTs-TPP, SWNTs-RuTPP, and SWNTs-FeTPP) and (b) PCA plot (PC2 vs. PC3) of 7 sensors showing well separated clusters for 5 VOCs under test (MeOH, EtOH, MEK and acetone).